Estimation of the synaptic input under a single cell model

Author: Mohammad Mahdi Hajimoradkhani
Scientific Director: Antoni Guillamon Grabolosa

ESCI-BDBI, Passeig de Pujades, 1, 08003 Barcelona
UPC Department of Mathematics, Campus Diagonal Sud, Carrer de Pau Gargallo, 14,
08028 Barcelona

Abstract

Individual neurons can be represented as mathematical objects such as dynamical systems, enabling the study of their electrical activity as a function of different biological parameters, time and most significantly different synaptic inputs. Using the Morris-Lecar model, which predicts the voltage of a neuron using electrical conductances of ionic channels and the conductances of inhibitory and excitatory synapses, it is possible to study the behaviour of a neuron under different inputs and the arising transformations of electrical activity based off changes in these inputs. Further, the model allows the estimation of the synaptic input a neuron is receiving based on its electrical activity. Under an experimental setting, the electrical activity(voltage) of a neuron can be measured with respect to time, however, the input the neuron receives to emit a certain behaviour remains difficult to determine experimentally, lending importance to this computational approach to estimate the input given a set of voltages. In pathological studies, evidence demonstrates a strong correlation between synapse dysfunction and neurodegenerative and neurodevelopmental diseases, and thus making it biologically significant to develop computational pipelines that allow the estimation of the synaptic input based on measurable experimental data. In this project, a series of simulations are prepared using the Morris-Lecar model, and a set of mathematical theories and transformations are applied which lead to the result that a neuronal dynamical system's electrical behaviour is equivalent when electrical inputs vary in short and long time intervals; as well as the result that the total synaptic input can be accurately estimated. However, the current solutions to the open problem of estimating the excitatory and inhibitory synaptic inputs, which are components of the total synaptic input, remain inaccurate.

Introduction

In the nervous system, it is often the case that neurons exhibit similar or identical physiological and electrophysiological properties, while simultaneously exhibiting qualitatively different electrical activity**[1].** To address this phenomena, families of models of varying complexity and dimensionality have been introduced, such as the Hodgkin-Huxley model**[2]**, which represent an individual neuron as a dynamical system. In such a representation, the electrical activity of the neuron is measured as a function of conductances of a variety of ionic channels, as well as the conductances of input excitatory and inhibitory synapses. This representation establishes a relationship between the behaviour of the neuron as a system based on its input, and inversely, from the behaviour of the system an inference could be made on the input.

Experimentally, there exist methods to determine the electrical activity of a neuron **[3]**, however, measurement of the input remains difficult. In tandem with this fact, recent research indicates a relationship between neurological disorders and abnormal synaptic behaviour **[4]**, making it a significant and growing topic of interest to estimate the synaptic input of a neuron. Therefore, the goal of this project is the estimation of the total synaptic input given a measurable quantity such as the temporal voltage. Additionally, the disentanglement of the synaptic input's constituent components, the excitatory and inhibitory inputs, is a key open problem the project attempts to tackle, as its solution would provide insight into the architecture of the brain. In order to emulate the experimental processes that produces voltage data, a computational pipeline that produces simulated voltage data based on the Morris Lecar model **[5]** is introduced.

The two dimensional Morris Lecar model, a relatively simple model which retains key properties, such as the neuron spiking capacity, as well as the conductances and equilibrium potentials of the calcium and potassium membrane channels, is used in this project to prepare a series of simulations to facilitate the estimation of the total synaptic input and then the excitatory and inhibitory conductances. In the general computational pipeline, the model is first fed with a set of simulated temporal conductances, yielding a set of temporal voltages as an output. The set of output voltages from these simulations are then used to estimate the synaptic input for each unit of time, and consequently, this estimation is compared with the real input values used to simulate the voltages. Following the estimation of the total synaptic input, the same pipeline is applied to estimate the excitatory and inhibitory synaptic conductances; the estimation of the excitatory and inhibitory conductances is a more challenging inverse problem **[6]** mathematically in contrast to estimation of the total synaptic input.

Materials and Methods

All the methods can be found in the script **ML_Sim_Filter.py** at the github repository:

https://github.com/mahdiESCI/FDP/tree/main/mahdiTFG

For visualisation, it is recommended to run the script **ML_Sim_Filter.ipynb** which is in compressed format on the repository.

1. Morris-Lecar model

The Morris-Lecar system consists of the equations:

$$\textbf{(1)}\frac{dV}{dt}=\frac{f(v,w)+I}{C_m} \mid f(v,w)=-(I_L+I_{Ca}+I_k), I=I_{app}+I_{syn}$$

$$\textbf{(2)}\frac{dW}{dt}=g(v,w) \mid g(v,w)=\frac{\phi(W_\infty-W)}{\tau_W}$$

$$\textbf{(3)}I_{syn}=g_E(v_E-v)+g_I(v_I-v)$$

$$I_L=g_L(v-v_L), I_K=g_K w(v-v_k)$$

$$I_{Ca}=g_{Ca}M_\infty(v-v_{Ca}) \mid M_\infty=\frac{1}{2}(1+\tanh\left[\frac{V-V_1}{V_2}\right])$$

$$W_\infty=\frac{1}{2}(1+\tanh\left[\frac{V-V_3}{V_4}\right]), \tau_W=\cosh\left[\frac{V-V_3}{2V_4}\right]$$

Component	Description
V	Membrane potential (Variable)
W	Recovery variable (Variable)
g_E	Excitatory conductance
g_I	Inhibitory conductance
g_L	Leak channel conductance
g_{Ca}	Calcium channel conductance
g_K	Potassiun channel conductance
I_{app}	Baseline applied currebnt
Cm	Membrane capacitance
$v_K, v_L, v_{Ca}, v_E, v_I$	Equirlibrium potential of respective channels
V_1, V_2, V_3, V_4	Tuning parameters

Table 1. Morris Lecar system variables and parameters. Brief description of the two variables and additional parameters of the Morris Lecar system.

The usage of the Morris Lecar model is such that in the computational pipeline, for each unit of time, it receives as input a set of g_E and g_I values which are used to compute $\frac{dV}{dt}$ and $\frac{dW}{dt}$. The euler integration method is then used to integrate sets of $\frac{dV}{dt}$ and $\frac{dW}{dt}$

values iteratively to obtain V and W.

$$V_n = V_{n-1} + hf(v,w), W_n = W_{n-1} + hg(v,w) \mid h = 0.01$$

Consequently, the values of V and W for a given simulation are fed to the robust exact filtering differentiator to obtain the estimations $\hat{V}, \hat{W}, \hat{V'}, \hat{V''}$ .These estimated values are then fitted to the equations of the Morris-Lecar system, in order to solve for the **Synaptic Input.** For the **Estimation of inhibitory and excitatory inputs**, $\hat{g}_E$ and $\hat{g}_I$, the same schema is applied.

2. Synaptic Input

From equation **(1)** that $I = I_{app} + I_{syn}$**,** each simulation of the neuron under the Morris-Lecar model is considered independent from the others based on the baseline applied current, I_{app} , and type of I_{syn} being fed to the system. In the different simulations produced, two distinct types of I_{syn}were given as input to the system; in one type the temporal g_E and g_I pairs have a slow variation with respect to time, and in the other type, the g_E and g_I values fluctuate faster. The set of temporal g_E and g_I values with relatively faster fluctuation come from a data file emulating realistic cortical activity, while the slower type was generated through taking the maximum and minimum values of the fast fluctuation set, and sampling g_E and g_I values from between the intervals formed by $g_{E_{min}}, g_{E_{max}}$ and $g_{I_{min}}, g_{I_{max}}$**.** Each sampled pair of g_E and g_I was held constant for time intervals of a fixed size, and as a result creating a slow variation input compared to the faster fluctuation set where g_E and g_I vary for all almost all units of time.

In addition to the two I_{syn} types, namely fast and slow input types, I_{app} values were chosen from the set $\{35,40,45,50,\}$to investigate the different states of the system resulting from different baseline applied currents, and to identify any inaccuracy introduced to the estimation of I_{syn} as a consequence of the baseline applied current.

For the estimation of g_E and g_I, the Morris Lecar system used to generate the temporal voltages was fed with the same constant g_E and g_I values such that $g_E = 0.071$ and $g_I = 0.362$ for all units of time.

3. Robust exact filtering differentiator

Given a signal, the robust exact filtering differentiator**[7]** retrieves the signal while discriminating noise in the signal, in addition to returning the derivatives of the given signal. In this applied context, for each unit of time, the robust exact filtering differentiator takes as input the temporal voltage obtained from the simulations of the Morris-Lecar model and returns the filtered V,$\frac{dV}{dt}$and $\frac{d^2V}{dt^2}$ for all units of time considered. The implementation of the filter takes as input the vector $[a_1, a_2, v_0, v_0^{'}, v_0^{''}]$ and returns the vector $[\hat{a}_1, \hat{a}_2, \hat{v}, \hat{v}^{'}, \hat{v}^{''}]$such that a_1 and a_2 are auxiliary variables.

$$\hat{a}_1 = -\lambda_4 L^{1/5} \left| a_1^{4/5} \right| sgn(a_1) + a_2$$
$$\hat{a}_2 = -\lambda_3 L^{2/5} \left| a_1^{3/5} \right| sgn(a_1) + v_0$$
$$\hat{v} = -\lambda_2 L^{3/5} \left| a_1^{2/5} \right| sgn(a_1) + v_0^{'}$$
$$\hat{v}^{'} = -\lambda_1 L^{4/5} \left| a_1^{1/5} \right| sgn(a_1) + v_0^{''}$$
$$\hat{v}^{''} = -\lambda_0 L sgn(a_1)$$

Note that sgn represents the sign function and λ_i and L are constants. Effectively, given an initial condition and a signal, which in this case is the temporal voltage, the robust exact differentiator returns the estimations $\hat{v}, \hat{v}^{'}$ and $\hat{v}^{''}$ which are used first in the **Estimation of total synaptic input**, and subsequently, the estimations are used for the voltages generated by the **constant** $g_E$and g_I simulation for **Estimation of inhibitory and excitatory inputs**, i.e. $\widehat{g_E}$and $\widehat{g_I}$.

4. Effective estimation of input

4.1. Estimation of total synaptic input

Equation **(1)** of the Morris-Lecar system can be rewritten in terms of I_{syn}**,**

$$I_{syn} = C_m \frac{dV}{dt} - (f(v, w) + I_{app})$$

For a given simulation, this equation can be fitted with the values of $\hat{v}, \hat{v}^{'}$ returned by the **Robust exact filtering differentiator** to estimate $\hat{I}_{syn}$ where:

$$\hat{I}_{syn} = C_m \hat{v}' - (f(\hat{v}, w) + I_{app})$$

The $\hat{I}_{syn}$ values computed for all units of the simulation time are then compared against the real I_{syn} values. The I_{syn} values are computed with respect to equation **(3)** of the Morris Lecar model, using the values of the excitatory and inhibitory conductances as well as the voltage.

4.2.Estimation of inhibitory and excitatory inputs

Derivating equation **(1)** of the Morris-Lecar system yields the second derivative of the temporal voltage. The first derivative of the system and the second derivative can together be considered under the system:

$$\textbf{(1)} \frac{dV}{dt} = \frac{f(v, w) + I}{Cm}$$

$$\textbf{(2)} \frac{d^2V}{dt^2} = \frac{1}{C_m}\left(\frac{\partial f}{\partial v}\frac{dV}{dt} + \frac{\partial f}{\partial w}\frac{dW}{dt} + I'_{syn}\right)$$

In order to obtain the estimations of the excitatory and and inhibitory inputs, $\widehat{g_E}$and $\widehat{g_I}$, the system can be rewritten in terms of $I'_{syn}$and I_{syn}.Given that **constant** $g_E$and g_I were used to generate the temporal voltages fed to the robust exact differentiator for the estimation of $\widehat{g_E}$and $\widehat{g_I}$, as mentioned in the methodology for the **Synaptic Input**, we have:

$$I'_{syn} = \frac{-dV}{dt}(g_E + g_I)$$

Meanwhile from the definition of I_{syn} from Morris Lecar equation **(3)** we know that:

$$I_{syn} = g_E(v_E - v) + g_I(v_I - v)$$

With respect to these definitions, the system can be rewritten in terms of $I'_{syn}$and I_{syn} as:

$$\textbf{(1)} g_E(v_E - v) + g_I(v_I - v) = C_m \frac{dV}{dt} - (f(v, w))$$

$$\textbf{(2)}\frac{-dV}{dt}(g_E+g_I)=C_m\frac{d^2V}{dt^2}-(\frac{\partial f}{\partial v}\frac{dV}{dt}+\frac{\partial f}{\partial v}\frac{dW}{dt})$$

Fitting the system with $\hat{v},\hat{v}'$and $\hat{v}''$ obtained from the **Robust exact filtering differentiator** results in:

$$\textbf{(1)}\hat{g}_E(v_E-\hat{v})+\hat{g}_I(v_I-\hat{v})=C_m\hat{v}r'-(f(\hat{v},w))$$
$$\textbf{(2)}-\hat{v}'(\hat{g}_E+\hat{g}_I)=C_m\hat{v}''-(\frac{\partial f}{\partial v}\hat{v}'+\frac{\partial f}{\partial v}\frac{dW}{dt})$$

Where the system formed by equations **(1)** and **(2)** could be solved for $\hat{g}_E$and $\hat{g}_I$ to obtain the excitatory and inhibitory conductances. The estimations are then compared against the real values, g_E and g_I , to measure accuracy. Note that:

$$\frac{\partial f}{\partial v}=-(g_L+g_{Ca}m'_\infty(v-v_{Ca})+g_{Ca}m_\infty+g_kw)$$
$$\frac{\partial f}{\partial w}=-g_K(v-v_K)$$

Results

1. Exploratory analysis

The behaviour of the system was equivalent for both the slow variation g_E and g_I sets and the relatively faster simulated set of conductances discussed in the **Synaptic Input** section of the methodology. This can be seen in the plots in **Figure 1** where the simulated neuron is spiking given the baseline applied current of $I_{app}=50$.

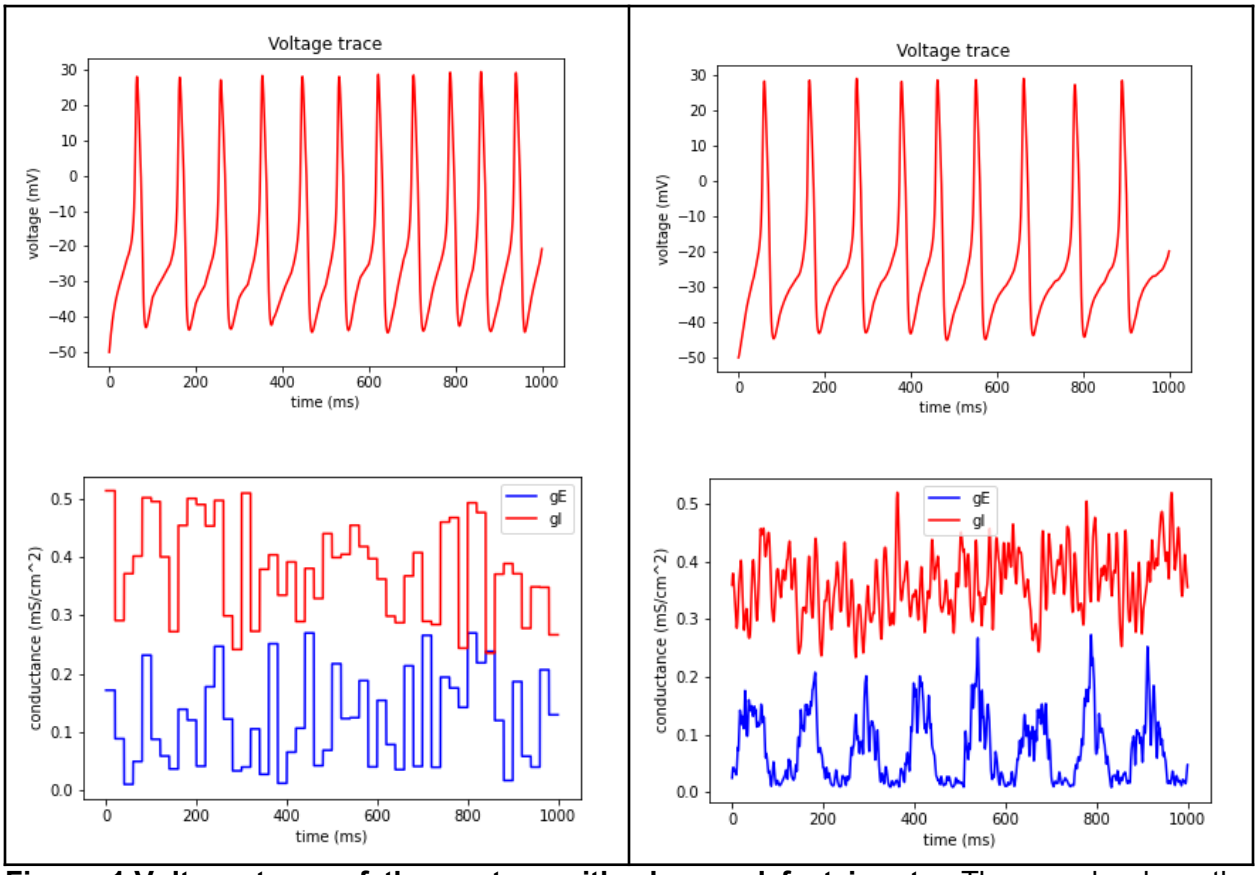

Figure 1.Voltage trace of the system with slow and fast inputs. The panels show the temporal electrical behaviour of the system i.e. the voltage trace, where the left panel represents the slow excitatory and inhibitory inputs and the right panel the fast inputs. $I_{app}=50$.

With respect to **Figure 2,t**he bifurcation diagram, which shows the voltage values the system visits as a function of its parameters, shows a type of bifurcation classified as SNIC(Saddle Node on Invariant Curve) bifurcation**[8]**, where at $I_{app}=40$ a limit cycle is born. For $I_{app}>40$, the system's temporal voltage displays oscillatory behaviour and the

neuron is spiking, whereas for I_{app}<40 it is in an inhibited state, as the voltage tends towards an attractor of the system.The data used to generate the bifurcation was compiled by the software XPPAUT**[9].** Note that the oscillatory behaviour on the bifurcation diagram corresponds to the spiking voltage traces in **Figure 1.**

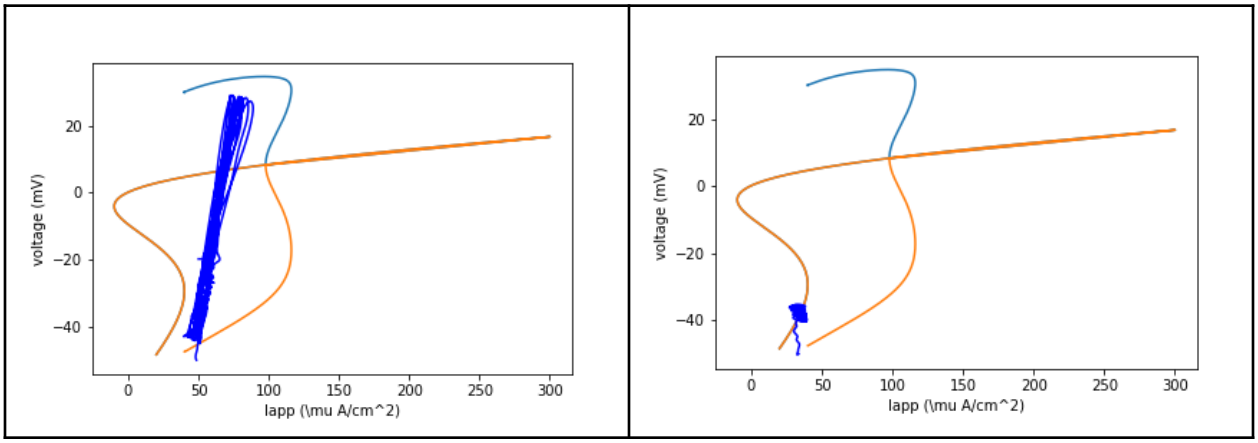

Figure 2.Oscillatory and quiescent states represented on the bifurcation diagram. Using the set of fast excitatory and inhibitory inputs, the temporal voltages were plotted on the bifurcation diagram, where in the left panel (oscillatory) $I_{app}=50$, and in the right (inhibited) $I_{app}=35$.

For both slow and fast excitatory and inhibitory inputs, the system displayed qualitatively equivalent behaviour on the bifurcation diagram, as can be seen in **Figure 3**. For the subcritical region i.e. I_{app}<40, for slow inputs, it was expected that if the system is given enough time it will rest perfectly on the attractor, given the generic behaviour of dynamical systems around attractors as $t \to \infty$**,**however this was not the case. In the supercritical region of I_{app}>40, for the slower inputs the system was expected to ride the limit cycle perfectly as well, and this was also untrue. The reason behind this observation is expanded upon in the discussion.

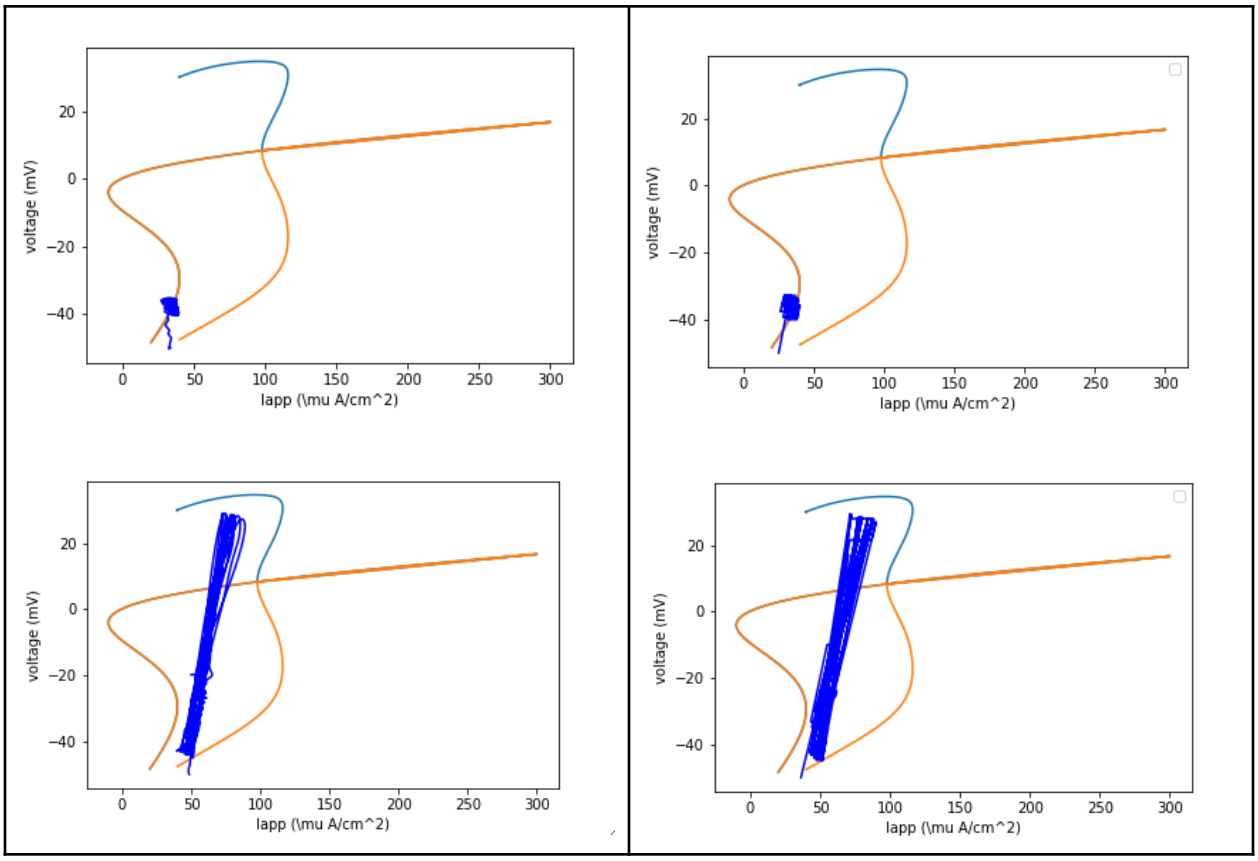

Figure 3. Bifurcation diagram for slow and fast inputs. At $I_{app} = 35$(top panels) and $I_{app} = 50$ (bottom panels), the behaviour of the system on the bifurcation diagram for the fast inputs(left panels) and slow inputs(right panels) is shown.

2. Estimation of the total synaptic input

Using the schema proposed in the **Estimation of total synaptic input** section of the methodology, the result of the estimation of the synaptic input can be found in **Figure 4.** For both the inhibited and oscillatory states, the estimation of the total synaptic input was successful, as can be seen through comparison of the trajectory of the true synaptic input computed from the simulated conductances with the estimation. Given that the behaviour of the system was shown to be equivalent for both slow and fast conductances, only the fast conductances mimicking real cortical activity were to obtain this result. The behaviour of the two states of the system for which the total synaptic input was estimated, namely the spiking and inhibited states, correspond to the behaviour shown on the bifurcation diagram in the left panels of **Figure 3.**

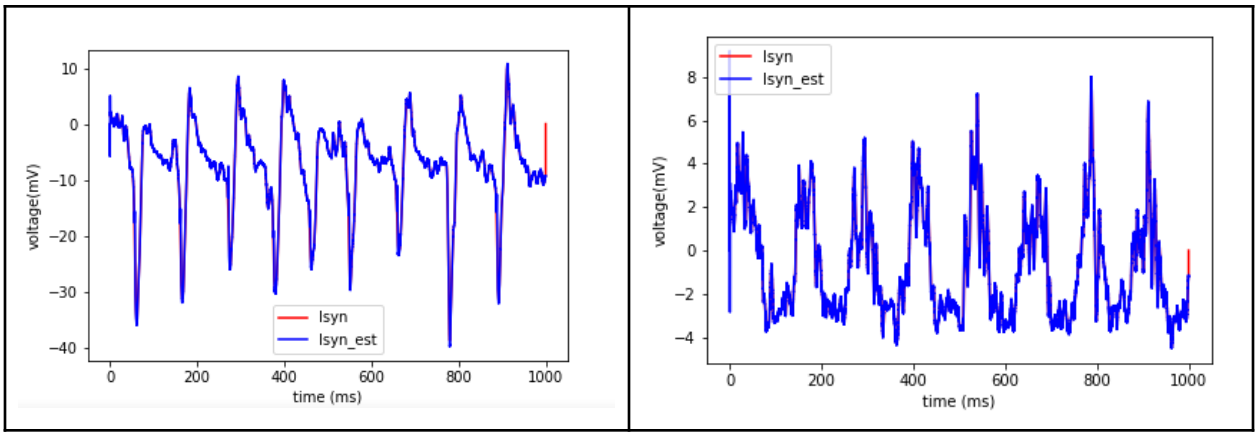

Figure 4. Estimation of the synaptic input plotted against the true synaptic input. The plots contain in blue the estimation of the synaptic input, and in red the true synaptic input for $I_{app} = 50$(left panel) and $I_{app} = 35$(right panel).

.

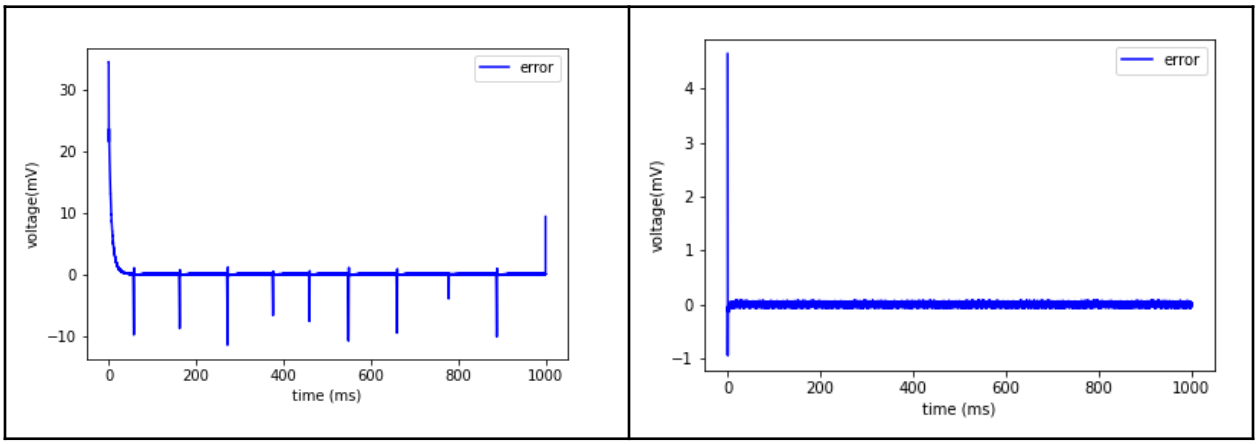

Figure 5. Error per unit of time for the estimation of the input. The difference between the true synaptic input and the estimation for $I_{app} = 50$(left panel) and $I_{app} = 35$(right panel).

The result of the estimation of the input for other simulations are not present as they exhibited the same qualitative behaviour. **Figure 5** shows the evaluation of the error for the estimations shown in **Figure 4.** It can be seen that when the neuron is in a spiking state, there are sporadic spikes in the error plot. This is due to the fact that in these instances, $\frac{dV}{dt}$ is zero, and the computation introduced in the **Estimation of total synaptic input** section diverges.

3. Estimation of inhibitory and excitatory conductances

The estimation of the excitatory and inhibitory conductances, g_E and g_I , did not produce accurate results as for the total simulation time considered, the estimations were either divergent from the true values or there was no solution to the system. While this result requires further mathematical evaluation, one plausible factor is that there are instances where $\frac{dV}{dt}$ is zero, and the consequence on equation **(2)** in the methodology section **Estimation of inhibitory and excitatory inputs** means that there is no solution to the system.

Discussion

Prior to the exploratory analysis, it was expected that for slow or constant input conductances, the temporal voltage would either perfectly ride on the limit cycle for I_{app}>40, or for the subcritical region i.e. I_{app}<40 sit perfectly on the attractor if given enough time. This is due to the fact that generically, dynamical systems tend to the attractors of the system if given some lagging input and enough time.The results obtained in the bifurcation diagrams for the slow input conductances proved this prediction wrong, and in turn revealed several key properties about the system. Given that the total synaptic input, I_{syn}, depends not only on the excitatory and inhibitory conductances but also the voltage, as shown in equation **(3)** of the Morris Lecar model, even for constant conductances the system will fluctuate; the voltage of the system gravitates around, but does not attach to the attractors of the system, making it dynamic in both the spiking state and the inhibited state. This also implies that for a given value of $g_E$and g_I, there could exist several values of I_{syn}, a notion that is not trivial and contributes to the complexity of solving the inverse problem of estimating the excitatory and inhibitory conductances. Fluctuations in g_E and g_I further contribute to the neuron represented by the system always being in a transient state, as I_{syn} will change too fast to reach the attractors of the system.

The total synaptic input was estimated with a satisfactory level of accuracy, while the estimation of g_E and g_I was divergent from the true values, due to the reason proposed in the results section **Estimation of inhibitory and excitatory conductances** as well as the inherent dynamic properties of the system. It is important to distinguish that in a real experimental setting, the real mathematical system that generated the temporal voltages is not known as the number of auxiliary variables is unknown a priori. However,

the computational pipeline remains robust as the robust exact filtering differentiator allows recovery of the filtered signal i.e. the voltage as well as its derivatives. Having access to these variables allows the implementation of models of even higher complexity like the Hodgkin-Huxley model to estimate the synaptic input, taking into account more electrophysiological properties, albeit at the cost of increased computational overhead. Dynamic clamp experiments**[10]** allow the injection of current into a cell given a temporal profile of g_E and g_I values, and are one way to produce a biological setting to test the computational pipeline.

In future work, it would be paramount to evaluate further why estimations of $g_E$and g_I diverge from the real values, and to introduce new mathematical techniques and systems to refine these estimations. Additionally, the methodology developed to compute the synaptic input for a single neruon could be integrated into network analysis of a population of simulated neuronal cells; the computational framework facilitates the estimation a neuron's synaptic input, and dynamical system models allow the simulation of the electrical activity of neurons which in turn lets us know their synaptic output. These two factors can be used to uncover properties of a network of neurons, but also provide a new framework for the estimation of the excitatory and inhibitory inputs based using a population of neurons rather than a single cell model.

Supplementary material

None.

Bibliography

[1]Izhikevic EM. Dynamical Systems in Neuroscience: The Geometry of Excitability and Bursting.

[2]Hodgkin AL, Huxley AF. A quantitative description of membrane current and its application to conduction and excitation in nerve. The Journal of Physiology. 1952;117(4):500–44.

[3]Fairless R, Beck A, Kravchenko M, Williams SK, Wissenbach U, Diem R, et al. Membrane Potential Measurements of Isolated Neurons Using a Voltage-Sensitive Dye. PLoS ONE. 2013;8(3).

[4]Lepeta K, Lourenco MV, Schweitzer BC, Martino Adami PV, Banerjee P, Catuara-Solarz S, et al. Synaptopathies: synaptic dysfunction in neurological disorders - A review from students to students. Journal of Neurochemistry. 2016;138(6):785–805.

[5]Lecar H. Morris-Lecar model. Scholarpedia. 2007;2(10):1333.

[6]Guillamon A, McLaughlin DW, Rinzel J. Estimation of synaptic conductances. Journal of Physiology-Paris. 2006;100(1-3):31–42.

[7]Levant A, Livne M. Robust exact filtering differentiators. European Journal of Control. 2020;55:33–44.

[8]Tsumoto K, Kitajima H, Yoshinaga T, Aihara K, Kawakami H. Bifurcations in Morris–Lecar neuron model. Neurocomputing. 2006;69(4-6):293–316.

[9]Ermentrout, B, Mahajan, A. Simulating, Analyzing, and Animating Dynamical Systems: A Guide to XPPAUT for Researchers and Students. Applied Mechanics Reviews. 2003;56(4).

[10]Berecki G, Verkerk AO, van Ginneken AC, Wilders R. Dynamic Clamp as a Tool to Study the Functional Effects of Individual Membrane Currents. Methods in Molecular Biology. 2014;:309–26.